Free vibration analysis of power-law and sigmoidal sandwich FG plates using refined zigzag theory

Aman Garg[*1], Simmi Gupta[2], Hanuman D. Chalak[2], Mohamed-Ouejdi Belarbi[3],
Abdelouahed Tounsi[4,5,6], Li Li[7] and A.M. Zenkour[8,9]

[1]*Department of Civil and Environmental Engineering, The NorthCap University,
Gurugram, Haryana,122017, India*
[2]*Department of Civil Engineering, National Institute of Technology Kurukshetra, Haryana, 136119, India*
[3]*Laboratoire de Recherche en Génie Civil, LRGC. Université de Biskra, B.P. 145, R.P. 07000, Biskra, Algeria*
[4]*YFL (Yonsei Frontier Lab), Yonsei University, Seoul, Korea*
[5]*Department of Civil and Environmental Engineering, King Fahd University of Petroleum &Minerals,
31261 Dhahran, Eastern Province, Saudi Arabia*
[6]*Material and Hydrology Laboratory, Faculty of Technology, Civil Engineering Department,
University of Sidi Bel Abbes, 22000 Sidi Bel Abbes, Algeria*
[7]*State Key Laboratory of Digital Manufacturing Equipment and Technology, School of Mechanical Science and
Engineering, Huazhong University of Science and Technology, Wuhan 430074, China*
[8]*Department of Mathematics, Faculty of Science, King Abdulaziz University, Jeddah, Saudi Arabia*
[9]*Department of Mathematics, Faculty of Science, Kafrelsheikh University, Kafrelsheikh, Egypt*

Abstract. Free vibration analysis of power law and sigmoidal sandwich plates made up of functionally graded materials (FGMs) has been carried out using finite element based higher-order zigzag theory. The present model satisfies all-important conditions such as transverse shear stress-free conditions at the plate's top and bottom surface along with continuity condition for transverse stresses at the interface. A Nine-noded C0 finite element having eleven degrees of freedom per node is used during the study. The present model is free from the requirement of any penalty function or post-processing technique and hence is computationally efficient. The present model's effectiveness is demonstrated by comparing the present results with available results in the literature. Several new results have been proposed in the present work, which will serve as a benchmark for future works. It has been observed that the material variation law, power-law exponent, skew angle, and boundary condition of the plate widely determines the free vibration behavior of sandwich functionally graded (FG) plate.

Keywords: free vibration; higher-order zigzag theory; power-law; sandwich FG plate; sigmoidal law

1. Introduction

Demerits related to laminated composite and sandwich plates such as delamination, matrix-fiber de-bonding, stress channeling effects (Garg and Chalak 2021a, b, Patni *et al.* 2018), etc.

∗Corresponding author, Assistant Professor, E-mail: amang321@gmail.com, amangarg@ncuindia.edu

opens the way for the new class of materials called functionally graded materials. In functionally graded materials (FGMs), material property regularly varies in a particular direction. Initially, FGMs were designed for constructing space structures, but due to their excellent properties, they are absorbed by various fields such as automobile, naval, civil, etc. Bending, free vibration, buckling, and transient are among the critical behaviors studied for sandwich functionally graded (FG) structures during preliminary stages.

Tornabene *et al.* (2015) presented detailed review of the differential quadrature-based finite element methods to analyze layered structures. Sayyad and Ghugal (2019) compiled the analysis work reported for the sandwich FG beams under various loading and environmental conditions. Zhang *et al.* (2019) summarized the available work related to analysis of FGM structures under bending, buckling and free vibration conditions. Ghatage *et al.* (2020) reported a review of the numerical modeling and analysis of multi-directional FGM structures. Garg *et al.* (2021a) presented detailed review on the analysis of sandwich FG structures.

Various theories are available for studying the free vibration behavior of sandwich plates. The most straightforward theory available for the free vibration analysis of sandwich FG plates is the classical laminated plate theory (CLPT). This theory neglects transverse deformation effects and hence overpredicts the value of frequencies (Garg and Chalak 2019). First-order shear deformation theory (FOSDT) assumes a constant transverse displacement field across the plate's thickness and cannot predict transverse shear stresses effectively (Carrera 2003). Tornabene (2009) carried out the free vibration behavior of annular plates using FOSDT. Thai *et al.* 2014 analyzed sandwich FG plates under free vibration conditions using FOSDT. Kurpa and Shmatko 2021 employed FOSDT for free vibration analysis of sandwich FG plates. To predict transverse shear stresses effectively, a shear correction factor is required (Birman and Bert 2002). The shear correction factor's value depends upon various parameters such as end conditions, material properties, the thickness of layers, etc. (Pai 1995, Bouafia *et al.* 2021).

The difficulties associated with FOSDT is handled efficiently by higher-order shear deformation theory (HOSDT). In HOSDTs, the displacement field is expressed in higher-order terms concerning the plate's thickness. Zenkour 2005a, b carried out vibration analysis of FG plates using trigonometric shear deformation theory and sinusoidal shear deformation theory. Also, a generalized theory was put forwarded by Zenkour for the analysis of FG plates (Zenkour 2006). Hadji *et al.* (2011) used HOSDT for the analysis of sandwich FG plates. However, the formulation neglects normal transverse strains during formulation. Neves *et al.* (2013) proposed meshless based HOSDT for bending, free vibration, and buckling analysis of sandwich FG plates. Mahi *et al.* (2015) carried out an analysis of sandwich FG plates using hyperbolic shear deformation theory. Bacciocchi *et al.* (2016) carried out a Gauss quadrature-based analysis of plates with variable thickness. Analysis of imperfect FGM plates under hygro-thermo-mechanical conditions was carried out by Daouadji *et al.* (2016). Bennoun *et al.* (2016) employed fifth-order shear deformation theory for the free vibration analysis of sandwich FG plates and derived exact solutions using Navier's solution. Meksi *et al.* (2019) proposed a hyperbolic shear deformation theory based on Navier solutions to analyze sandwich FG plates. Zouatnia and Hadji (2019) proposed closed form solutions for free vibration analysis of sandwich FG plates. Keddouri *et al.* (2019) proposed application of HOSDT for the analysis of porous FGM plates. Belalia *et al.* (2019) analyzed sandwich FG plates using the *p* version of the finite element method (FEM). To predict transverse behavior accurately, equilibrium equations were employed. Fu *et al.* (2020) carried out a free vibration analysis of sandwich FG plates using nth-order HOSDT along with the differential quadrature method. Singh and Harsha (2020) used non-linear HOSDT for vibration

analysis of sigmoidal sandwich FG plates resting on elastic foundation. Analytical solutions for analysis of sandwich FGM, beams based on HOSDT were published by Hadji and Bernard (2020). Ye *et al.* (2021) carried out a free vibration analysis of sandwich FG plates using HOSDT. Analytical solutions were derived using Navier's solutions. Hadji *et al.* (2021, 2022) employed parabolic shear deformation theory (SDT) for analysis of porous FGM plates. Saad *et al.* (2021) carried out free vibration analysis of porous sandwich FG plates. Wave propagation analysis in FGM plates using quasi 3D HOSDT was carried out by Tahir *et al.* (2022).

Burlayenko and Sadowski (2020), in their work, showed that stresses have nonlinear patterns across the thickness of sandwich FG plates. The nonlinear variation increases with an increase in the plate's metallic phase for plates made with a power law. However, these nonlinear stresses across the plate's thickness, especially at interfaces, cannot be predicted accurately by using HOSDT (Apetre *et al.* 2008, Brischetto 2009, Carrera *et al.* 2011). Another kind of theory called layerwise theory (LWT) can predict stresses efficiently. LWT's are of two types: discrete and refined LWTs. In discrete LWT, each layer is analyzed separately and then the results are integrated over the entire domain. Pandey and Pradyumna (2015) proposed FE based discrete LWT for the free vibration analysis of sandwich FG plates. Ferreira *et al.* (2013) carried out an analysis of sandwich plates using Gauss quadrature based LWT. As in case of discrete LWT, each layer is analyzed separately, and hence is computationally costly as with an increase in layers, the number of unknowns also increases. In refined LWTs (also called zigzag theories), the number of unknowns at each layer is expressed in unknowns at the reference plane (usually middle plane). This makes the number of unknowns at each layer independent of the number of layers.

Neves *et al.* (2012) reported bending behaviour of sandwich FG plates using hyperbolic zigzag theory and further extended for buckling analysis of sandwich FG plates (Neves *et al.* 2017). Iurlaro *et al.* (2014) and Di Sciuva and Sorrenti (2019) used HOZT for carrying out free vibration analysis of sandwich FG plates using the Ritz method in conjunction with Chebyshev polynomials. Garg *et al.* (2020a), Garg *et al.* (2021) analyzed exponential and power-law sandwich FG plates and beams using C-0 HOZT. The zigzag term was also included in the transverse displacement field, which helps predict thick sandwich plates' behavior efficiently. Dorduncu (2020) used the peridynamic operator based zigzag theory to analyze power-law and exponentially graded sandwich FG plates. Chen and Su (2021) presented analytical solutions in framework of HOZT for studying the behavior of sandwich FG beams. Chanda and Sahoo (2021) presented non-polynomial zigzag theory for analysis of sandwich plates. The choice of material homogenization rule widely affects the behavior of sandwich FGM structures (Garg *et al.* 2020b, 2021b, c).

Regarding the benefits of including zigzag effects and normal transverse stresses, Brischetto and his co-authors (Brischetto 2009, Carrera *et al.* 2011) and Zenkour and his co-authors (Zenkour *et al.* 2009, Zenkour 2009) stated, "Refinements of classical theories that include additional in-plane variables could result meaningless unless transverse normal strain effects are taken into account". Linear 3D Elasticity based solutions for power-law sandwich FGM is carried out by Li *et al.* (2008). Liu *et al.* (2015) used FOSDT for face sheets and 3D elasticity solutions for the core for analyzing sandwich FG plates. 3D elasticity-based solutions are the most accurate but are computationally costly.

In the present work, free vibration analysis of sandwich FG plates (non-skew and skew) is carried out using recently proposed HOZT (Chalak *et al.* 2012). The third-order variation of the in-plane displacement field is taken along with the variation of the transverse displacement field across the plate's thickness. The zigzag effects are introduced using a linear unit Heaviside step function. The present theory satisfies interlaminar transverse stress continuity at the interface and

zero condition at the plate's top and bottom surfaces for transverse shear stresses. Nine-noded C_0 FE having twelve degrees of freedom per node is used during analysis. The present model does not require penalty approach or post-processing technique and hence is computationally more efficient. A comparative study has been carried out on the free vibration behavior of sandwich FG plates made of power-law and sigmoidal homogenization rules. Present results are validated with available results in the literature. Several new results are also given, especially for sigmoidal sandwich FG plates, which will serve as the benchmark for future studies.

2. Mathematical and material modeling

Governing Equation: The equation of motion of the beam/plate system can be obtained by applying Hamilton's principle

$$\delta \int_0^t (T - U)dt = 0 \tag{1}$$

In the above Eq. (1), the work done by external forces is neglected and the damping is also not considered. The Hamilton's principle leads to the following equilibrium equation of a system

$$[K']\{\psi\} = \omega^2 [M]\{\psi\} \tag{2}$$

Considering a plate made up of FGM lying in X-Y plane. The thickness of plate lies along the Z-axis as shown in Fig. 1. The variation of in-plane displacement (along x-direction) across the thickness of a sandwich FG plate may be expressed as follows (Chalak *et al.* 2012)

$$U = u_0 + z\theta_x + \sum_{i=1}^{n_u-1}(z - z_i^u)H(z - z_i^u)\alpha_{xu}^i + \sum_{j=1}^{n_l-1}(z - z_i^l)H(-z + z_i^l)\alpha_{xl}^j + \beta_x z^2 + \eta_x z^3 \tag{3}$$

Similarly, the in-plane displacement along the y-direction is expressed as

$$V = v_0 + z\theta_y + \sum_{i=1}^{n_u-1}(z - z_i^u)H(z - z_i^u)\alpha_{yu}^i + \sum_{j=1}^{n_l-1}(z - z_i^l)H(-z + z_i^l)\alpha_{yl}^j + \beta_y z^2 + \eta_y z^3 \tag{4}$$

where, u_0 and v_0 denotes the in-plane displacements of the mid surface, θ_x and θ_y are the rotations of the normal to the middle plane about the y- axis and x- axis respectively, n_u and n_l are number of upper and lower layers respectively, β_x, β_y, η_x and η_y are the higher order unknown terms, $\alpha_{xu}^i, \alpha_{xl}^j, \alpha_{yu}^i$, and α_{yl}^j are the slopes of *i*-th/*j*-th layer interfaces corresponding to upper and lower layers respectively and $H(z - z_i^u)$ and $H(-z + z_i^u)$ are the unit step functions.

The transverse displacement is assumed to vary quadratically through the core thickness and constant over the face sheets and it may be expressed as

$$W = \begin{cases} l_1 w_u + l_2 w_0 + l_3 w_l & \text{for core} \\ w_u & \text{for upper face layers} \\ w_l & \text{for lower face layers} \end{cases} \tag{5}$$

where w_u, w_0, and w_l are the values of the transverse displacement at the top, middle and bottom of the core layer respectively; and l_1, l_2 and l_3 are Lagrangian interpolation functions in the thickness co-ordinate which can be expressed as

$$l_1 = \frac{z(z+h_l)}{h_u(h_u+h_l)}, l_2 = \frac{(z+h_l)(h_u-z)}{h_u h_l}, l_3 = \frac{z(-z+h_u)}{-h_l(h_u+h_l)} \tag{6}$$
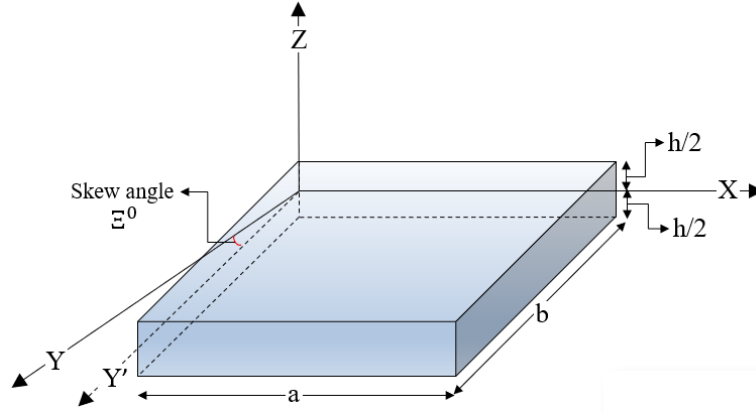
Fig. 1 Geometry of skew sandwich FG plate

The stress-strain relationship of an orthotropic layer/ lamina (say *k*-th layer) having any fiber orientation with respect to structural axes system (x-y-z) may be expressed as

$$\{\bar{\sigma}\} = [\bar{Q}]_k\{\bar{\varepsilon}\} \tag{7}$$

where $\{\bar{\sigma}\}$, $\{\bar{\varepsilon}\}$ and $[\bar{Q}]_k$ are the stress vector, the strain vector, and the transformed rigidity matrix of *k*-th lamina, respectively.

The strain vector $\{\bar{\varepsilon}\}$ in the above equation may be expressed in terms of displacement components as

$$\{\bar{\varepsilon}\} = \left[\frac{\partial U}{\partial x} \quad \frac{\partial V}{\partial y} \quad \frac{\partial W}{\partial z} \quad \frac{\partial U}{\partial y} + \frac{\partial V}{\partial x} \quad \frac{\partial U}{\partial z} + \frac{\partial W}{\partial x} \quad \frac{\partial V}{\partial z} + \frac{\partial W}{\partial x}\right] \tag{8}$$

Utilizing the following conditions: $\left(\sigma_{xz} = \sigma_{yz} = 0 \text{ at } z = \pm h/2\right)$, $\left(\sigma_{xz}^i = \sigma_{xz}^{i+1} \text{ and } \sigma_{xz}^i = \sigma_{xz}^{i+1}\right)$ at the interfaces, $U = u_u$ and $V = v_u$ at the top and $U = u_l$ and $V = v_l$ at the bottom of the plate, β_x, β_y, η_x, η_y, α_{xu}^i, α_{xl}^j, α_{yu}^i, α_{yl}^j, $(\partial w_u/\partial x)$, $(\partial w_l/\partial x)$, $(\partial w_u/\partial y)$ and $(\partial w_l/\partial y)$ may be expressed in terms of the displacements u_0, v_0, θ_x, θ_y, u_u, v_u, u_l and v_l as

$$\{B\} = [A]\{\alpha\} \tag{9}$$

where, $\{B\} = \{\beta_x \ \beta_y \ \eta_x \ \eta_y \ \alpha_{xu}^1 \ \alpha_{xu}^2 \ ... \ \alpha_{xu}^{n_u-1} \ \alpha_{xl}^1 \ \alpha_{xl}^2 \ ... \ \alpha_{xl}^{n_l-1} \ \alpha_{xu}^1 \ \alpha_{xu}^2 \ ... \ \alpha_{xu}^{n_u-1} \ \alpha_{xl}^1 \ \alpha_{xl}^2 \ ...$
$\alpha_{xl}^{n_l-1} (\partial w_u/\partial x) (\partial w_l/\partial x) (\partial w_u/\partial y) (\partial w_l/\partial y)\}^T$, $\{\alpha\} = \{u_0 \ v_0 \ \theta_x \ \theta_y \ u_u \ v_u \ u_l \ v_l\}^T$ and the elements of $[A]$ are dependent on material properties. It is to be noted that last two entries of the vector $\{B\}$ helps to define the derivatives of transverse displacement at the top and bottom faces of the plate in terms of the displacements u_0, v_0, w_0, θ_x, θ_y, u_u, v_u, w_u, u_l, v_l, and w_l to overcome the problem of C$_1$ continuity as mentioned before.

Using the above equations, the in-plane displacement fields as given in Eqs. (3) and (4) may be expressed as

$$\begin{aligned} U &= b_1 u_0 + b_2 v_0 + b_3 \theta_x + b_4 \theta_y + b_5 u_u + b_6 v_u + b_7 u_l + b_8 v_l \\ V &= c_1 u_0 + c_2 v_0 + c_3 \theta_x + c_4 \theta_y + c_5 u_u + c_6 v_u + c_7 u_l + c_8 v_l \end{aligned} \tag{10}$$

where, the coefficients *bi's* and *ci's* are function of thickness coordinates, unit step functions and material properties.

The generalized displacement vector $\{\delta\}$ for the present plate model can now be written with the help of Eqs. (9) and (10) as

$$\{\delta\} = \left\{u_0 \; v_0 \; w_0 \; \theta_x \; \theta_y \; u_u \; v_u \; w_u \; u_l \; v_l \; w_l\right\}^T \tag{11}$$

Using linear strain-displacement relation and Eqs. (8) - (11), the strain vector may be expressed in terms of unknowns (for the structural deformation) as

$$\{\bar\varepsilon\} = \left[\frac{\partial U}{\partial x} \; \frac{\partial V}{\partial y} \; \frac{\partial W}{\partial z} \; \frac{\partial U}{\partial y} + \frac{\partial V}{\partial x} \; \frac{\partial U}{\partial z} + \frac{\partial W}{\partial x} \; \frac{\partial V}{\partial z} + \frac{\partial W}{\partial x}\right] \text{ or } \{\bar\varepsilon\} = [H]\{\varepsilon\} \tag{12}$$

where,

$$\{\varepsilon\} =$$
$$\{u_0 \; v_0 \; w_0 \; \theta_x \; \theta_y \; u_u \; v_u \; w_u \; u_l \; v_l \; w_l \; (\partial u_0/\partial x) \; (\partial u_0/\partial y) \; (\partial v_0/\partial x) \; (\partial v_0/\partial y) \; (\partial w_0/\partial x)$$
$$(\partial w_0/\partial y) \; (\partial \theta_x/\partial x) \; (\partial \theta_x/\partial y) \; (\partial \theta_y/\partial x) \; (\partial \theta_y/\partial y) \; (\partial u_u/\partial x) \; (\partial u_u/\partial y) \; (\partial v_u/\partial x)$$
$$(\partial v_u/\partial y) \; (\partial w_u/\partial x) \; (\partial w_u/\partial y) \; (\partial u_l/\partial x) \; (\partial u_l/\partial y) \; (\partial v_l/\partial x) \; (\partial v_l/\partial y) \; (\partial w_l/\partial x) \; (\partial w_l/\partial y)\}$$

and the elements of $[H]$ are functions of z and unit step functions.

In the present problem, a nine-node quadratic element with eleven field variables (u_0, v_0, w_0, θ_x, θ_y, u_u, v_u, w_u, u_l, v_l, and w_l) per node is employed.

Using the finite element method, the generalized displacement vector $\{\delta\}$ at any point may be expressed as (Garg and Chalak 2021a)

$$\{\delta\} = \sum_{i=1}^{n} N_i\{\delta\}_i \tag{13}$$

where, $\{\delta\}_i$ is the displacement vector corresponding to node i, N_i is the shape function associated with the node i.

The strain vector $\{\varepsilon\}$ that appeared in Eq. (12) may be expressed in terms of unknowns (for the structural deformation) using Eq. (13) as

$$\{\varepsilon\} = [B]\{\delta\} \tag{14}$$

where [B] is the strain-displacement matrix in the Cartesian coordinate system.

The consistent mass matrix can be derived as that of stiffness matrix. The acceleration vector at any point within the laminated plate structure may be expressed as

$$\{d^2\bar\psi/dt^2\} = \begin{Bmatrix} d^2U/dt^2 \\ d^2V/dt^2 \\ d^2W/dt^2 \end{Bmatrix} = -\omega^2 \begin{Bmatrix} U \\ V \\ W \end{Bmatrix} = -\omega^2[F]\{\psi\} \tag{15}$$

where matrix $[F]$ of order 3×11 contains z terms and some constant quantities as that of *[H]*.

$$[M_e] = \sum_{i=1}^{n_u+n_l} \iiint \rho_i [N]^T [F]^T [N][F] dx dy dz = \iint [N]^T [L][N] dx dy \tag{16}$$

where ρ_i is the mass density of the i-th layer and the matrix $[L]$ is

$$[L] = \sum_{i=1}^{n_u+n_l} \int \rho_i [F]^T [F] dz \tag{17}$$

For skew plate it is assumed that the plate is skew with respect to the Y-axis only (Fig. 1). Therefore, the stiffness matrix for the elements lying on the skew edges must be transformed from the local axis (X-Y-Z) to the global axis (X-Y'-Z), which is carried out using the simple transformation rules can be stated as (Chalak *et al.* 2014)

$$\{\delta^1\}^T = [T_N]\{\delta\}^T \tag{18}$$

Table 1 Material homogenization laws

Nomenclature	Faces			$V_c(z)$			Fig. No.
	Bottom	Core	Top	$z \in [h_0, h_1]$	$z \in [h_1, h_2]$	$z \in [h_2, h_3]$	
H-Type-A	FGM	Ceramic	FGM	$\left(\frac{z-h_0}{h_1-h_0}\right)^n$	1	$\left(\frac{z-h_3}{h_2-h_3}\right)^n$	2(a)
S-Type-A	FGM	Metal	FGM	$1 - \left(\frac{z-h_0}{h_1-h_0}\right)^n$	0	$1 - \left(\frac{z-h_3}{h_2-h_3}\right)^n$	2(b)
CT-Type-B	Metal	FGM	Ceramic	0	$\left(\frac{z-h_1}{h_2-h_1}\right)^n$	1	3(a)
MT-Type-B	Ceramic	FGM	Metal	1	$1 - \left(\frac{z-h_1}{h_2-h_1}\right)^n$	0	3(b)
H-Type-S	FGM	Ceramic	FGM	$0.5\left(\frac{z-h_0}{h_{m1}-h_0}\right)^n$ for $z \in [h_0, h_{m1}]$ where $h_{m1} = (h_0 + h_1)/2$ $1 - 0.5\left(\frac{z-h_1}{h_{m1}-h_1}\right)^n$ for $z \in [h_{m1}, h_1]$	1	$1 - 0.5\left(\frac{z-h_2}{h_{m2}-h_2}\right)^n$ for $z \in [h_2, h_{m2}]$ where $h_{m2} = (h_2 + h_3)/2$ $0.5\left(\frac{z-h_3}{h_{m2}-h_3}\right)^n$ for $z \in [h_{m2}, h_3]$	4(a)
S-Type-S	FGM	Metal	FGM	$1 - V_c(z)$ for H-Type-S	0	$1 - V_c(z)$ for H-Type-S	4(b)

where $[T_N]$ is the node transformation matrix and $\{\delta^1\}$ is displacement vector in the localized coordinate system.

Material Homogenization laws adopted during the present study are power-law and sigmoidal laws. These laws are summarized in Table 1. Material properties used during the present study are: Metallic phase is made up of Aluminium (Al) $E = 70$ GPa, $\nu = 0.30, \rho = 2707$ kg/m^3. The ceramic phase is made up of Alumina (Al_2O_3) $E = 380$ GPa, $\nu = 0.30, \rho = 3800$ kg/m^3. The relationship used to convert the dimensional natural frequency to its non-dimensional form is as $\bar{\omega} = \omega a^2/h \times \sqrt{\rho_0/E_0}$ where $\rho_0 = 1$ kg/m^3, $E_0 = 1$ GPa.

In above table, *n* represents power-law coefficient which describes how the phase transformation will take place from metal to ceramic or vice versa. The symbols h_0, h_1, h_2, and h_3 represents the thickness of each layer as indicated in Figs. 2-4. The term *a/h* in the manuscript represents the thickness ratio (ratio of length of plate parallel to X-axis to its total thickness), and Ξ^0 represents the skew angle of the plate with respect to the Y-axis (Fig. 1). The thickness of each layer of the FGM is defined as 1-2-1 which represents the thickness of top face-core-bottom face i.e., the thickness of core is 2 times of that of face layers and the thickness of both the faces are same.

Boundary conditions: Following boundary conditions are used during the present study: Clamped end (C): All degrees of freedom are restrained. Free (F): All degrees of freedom are free. Simply supported (S): (parallel to X-axis) Degrees of freedom $u_0, v_0, w_0, \theta_x, u_u, w_u, u_l, w_l$ are allowed and θ_y, v_u, v_l are restrained at one edge, whereas on the opposite edge, w_0, w_u, w_l are restrained and other are free. For edges parallel to Y-axis: $u_0, v_0, w_0, \theta_y, v_u, w_u, v_l, w_l$ are allowed and θ_y, u_u, u_l are restrained, whereas on the opposite edge, w_0, w_u, w_l are restrained and other are free.

Fig. 2 Variation of Young's modulus across the thickness for 1-1-1 (a) H-Type-A and (b) S-Type-A sandwich FG plate

3. Results and discussion

Convergence study: To choose an appropriate mesh size, a convergence study is carried out firstly. The convergence study is carried out on Type-A 1-1-1, simply supported sandwich plate (a/h=100). Results for convergence of non-dimensional natural frequency ($\bar{\omega}$) are reported in Fig. 5. Present results converged at mesh size of 14×14. Therefore, in further studies, the same mesh size is taken.

Type-A sandwich FG plate: All-around simply supported Type-A sandwich FG plate is analyzed under free vibration conditions. Results for non-dimensional natural frequencies for H-Type-A and S-Type-A plates are reported in Table 2 for a/h=100 and 10 and n=0.5, 1, 5, and 10. Present results are compared with the 3D Elasticity based results given by Li *et al.* (2008) and CLPT, FOSDT, and various shear deformation theories (HOSDT, Sinusoidal shear deformation theory (SSDT)) published by Zenkour (2005b). Present results are in very good agreement with elasticity-based results for both H-Type-A and S-Type-A plates for both symmetric and unsymmetric thickness schemes. For unsymmetric thickness schemes (2-2-1, 2-1-1), the present model predicts non-dimensional natural frequency slightly on the higher side but more accurate than FOSDT and HOSDT. The CLPT overpredicts the non-dimensional natural frequency while FOSDT underpredicts non-dimensional natural frequency for H-Type-A plates. With increase in value of a/h, value of non-dimensional natural frequency decreases for both H-Type-A and S-Type-A plates. With increase in value of n, value of non-dimensional natural frequency decreases for H-Type-A plate and increases for S-Type-A plate. with increase in thickness of core, value of

(a)

(b)

Fig. 3 Variation of Young's modulus across the thickness for 1-1-1 (a) CT-Type-B and (b) MT-Type-B sandwich FG plate
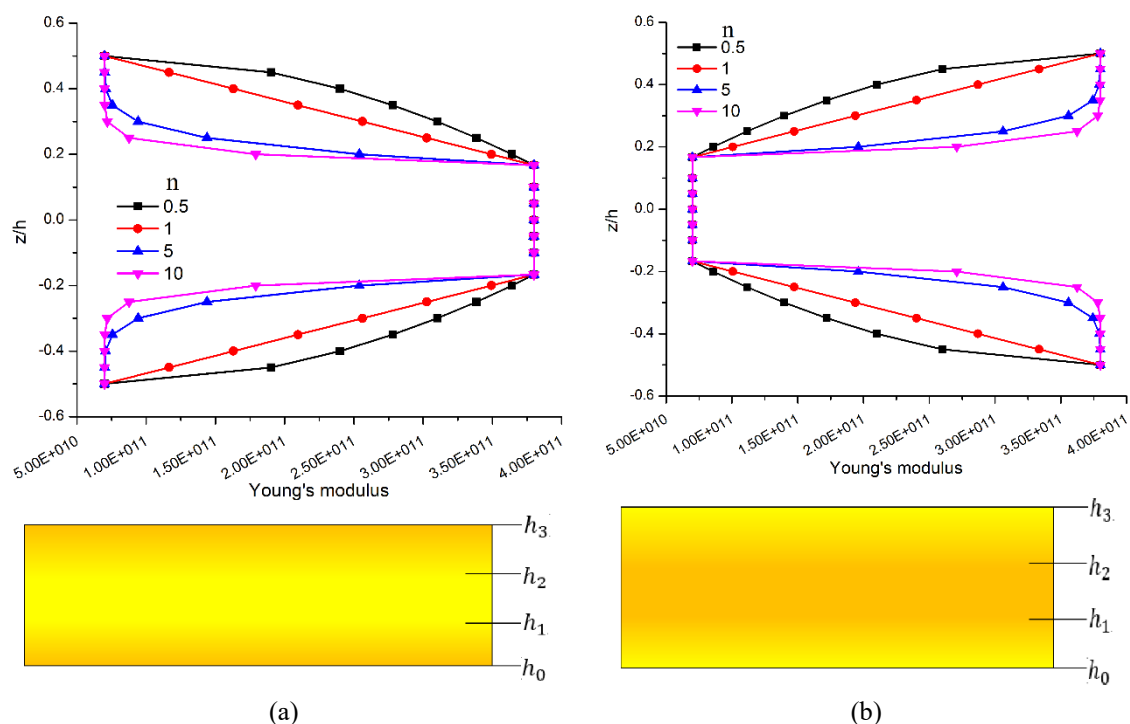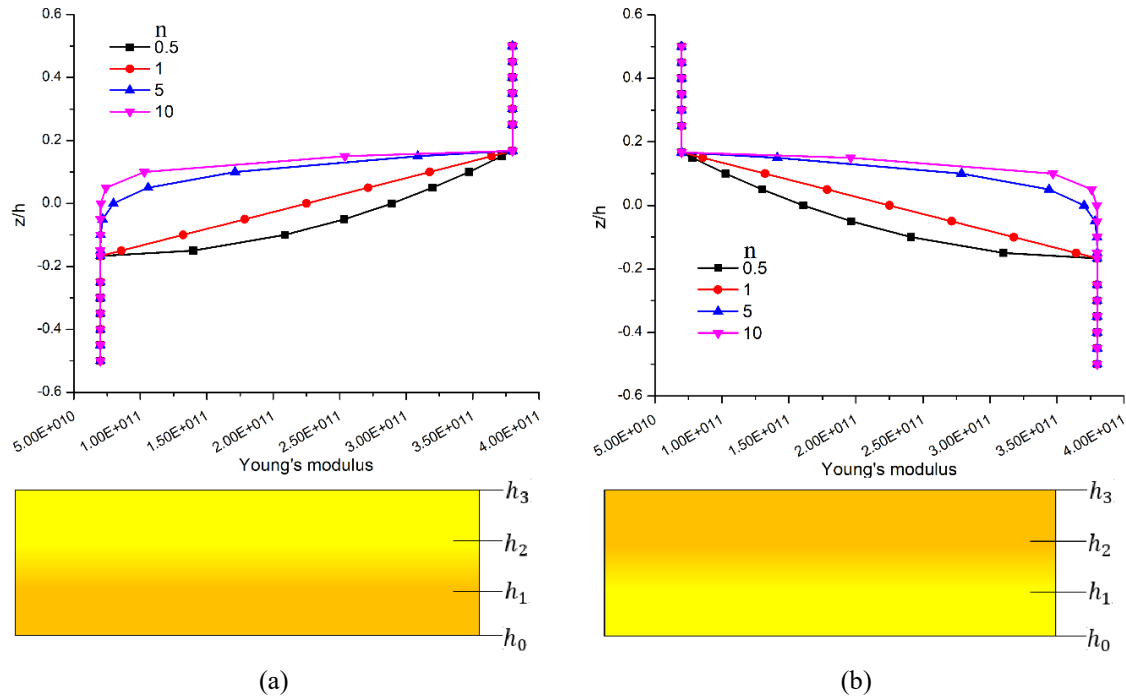

(a)

(b)
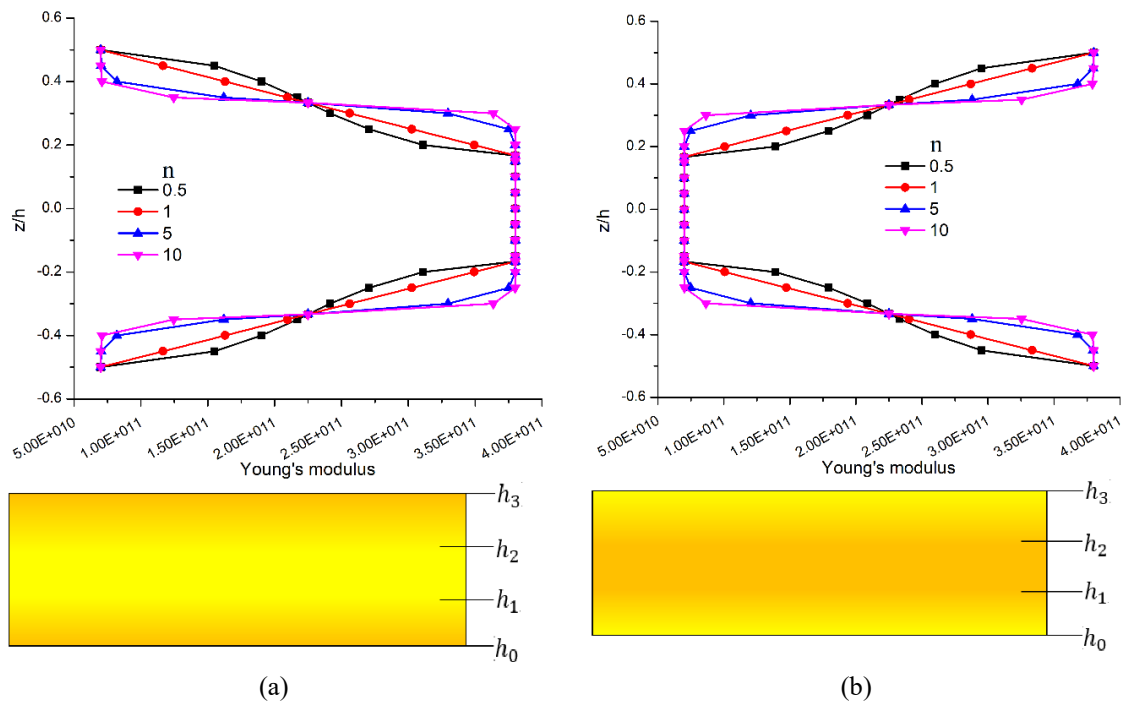
Fig. 4 Variation of Young's modulus across the thickness for 1-1-1 (a) H-Type-S and (b) S-Type-S sandwich FG plate

Aman Garg et al.
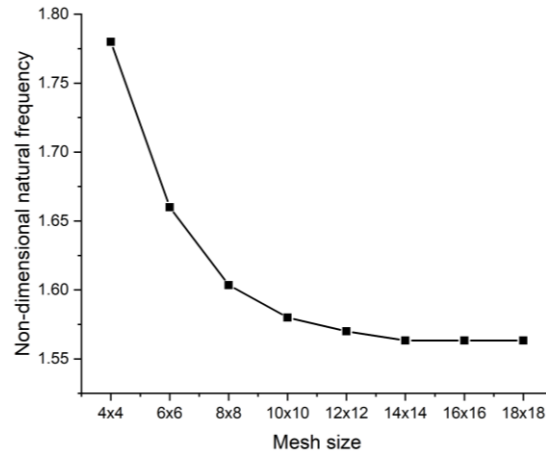
Fig. 5 Convergence study for SSSS H-Type-A sandwich plate (*a/h*=100, *n*=0.5)

Table 2 Variation of non-dimensional natural frequency for SSSS square-shaped Type-A sandwich FG plate

a/h	*n*	Source	2-1-2	2-1-1	1-1-1	2-2-1	1-2-1	1-8-1
		H-Type-A						
	0.5	Present	1.5398	1.5904	1.5634	1.6192	1.6102	1.7717
		3D Elasticity (Li *et al.* 2008)	1.5235	-	1.5604	1.5903	1.6191	1.7635
		% Error	1.070	-	0.192	1.817	-0.550	0.465
	1	Present	1.3455	1.4240	1.3848	1.4732	1.4766	1.7074
		3D Elasticity (Li *et al.* 2008)	1.3297	-	1.3851	1.4299	1.4755	1.6990
100		% Error	1.188	-	-0.022	3.028	0.075	0.494
	5	Present	0.9831	1.0988	1.0404	1.1464	1.2045	1.5651
		3D Elasticity (Li *et al.* 2008)	0.9990	-	1.0630	1.1302	1.1969	1.5698
		% Error	-1.592	-	-2.126	1.433	0.635	-0.299
	10	Present	0.9579	1.0549	1.0133	1.0952	1.1588	1.5408
		3D Elasticity (Li *et al.* 2008)	0.9593	-	1.0123	1.0806	1.1440	1.5416
		% Error	-0.146		0.099	1.351	1.294	-0.052
	0.5	Present	1.4865	1.5059	1.5290	1.5500	1.5945	1.7185
		3D Elasticity (Li *et al.* 2008)	1.4860	1.5084	1.5213	1.5492	1.5766	1.7113
		% Error	0.034	-0.166	0.506	0.052	1.135	0.421
		CLPT (Zenkour 2005b)	1.5124	1.5426	1.5490	1.5837	1.6072	-
		FOSDT (Zenkour 2005b)	1.4815	1.5103	1.5169	1.5500	1.5727	-
10		HOSDT (Zenkour 2005b)	1.4840	1.5125	1.5192	1.5519	1.5745	-
	1	Present	1.3037	1.3484	1.3600	1.3963	1.4590	1.6587
		3D Elasticity (Li *et al.* 2008)	1.3018	1.3351	1.3552	1.3976	1.4413	1.6511
		% Error	0.146	0.996	0.354	-0.093	1.228	0.460
		CLPT (Zenkour 2005b)	1.3202	1.3715	1.3752	1.4324	1.4649	-
		FOSDT (Zenkour 2005b)	1.2972	1.3463	1.3507	1.4055	1.4372	-
		HOSDT (Zenkour 2005b)	1.3001	1.3488	1.3533	1.4078	1.4393	-
		SSDT (Zenkour 2005b)	1.3002	1.3489	1.3533	1.4079	1.4393	-

Table 2 Continued

a/h	n	Source	2-1-2	2-1-1	1-1-1	2-2-1	1-2-1	1-8-1
10	5	Present	0.9842	1.0727	1.0269	1.1227	1.1811	1.5252
		3D Elasticity (Li *et al.* 2008)	0.9810	1.0294	1.0453	1.1098	1.1756	1.5299
		% Error	0.326	0.321	-1.760	1.162	0.468	-0.307
		CLPT (Zenkour 2005b)	0.9919	1.0879	1.0556	1.1619	1.1886	-
		FOSDT (Zenkour 2005b)	0.9787	1.0715	1.0418	1.1446	1.1715	-
		HOSDT (Zenkour 2005b)	0.9818	1.0743	1.0446	1.1473	1.1739	-
		SSDT (Zenkour 2005b)	0.9820	1.0744	1.0448	1.1474	1.1739	-
	10	Present	0.9412	1.0078	0.9979	1.0997	1.1197	1.5022
		3D Elasticity (Li *et al.* 2008)	0.9407	0.9892	0.9952	1.0610	1.1246	1.5033
		% Error	0.053	1.880	0.271	3.648	-0.436	-0.073
		CLPT (Zenkour 2005b)	0.9524	1.0518	1.0052	1.1188	1.1361	-
		FOSDT (Zenkour 2005b)	0.9396	1.0358	0.9925	1.1026	1.1206	-
		HOSDT (Zenkour 2005b)	0.9429	1.0386	0.9955	1.1053	1.1231	-
		SSDT (Zenkour 2005b)	0.9433	1.0455	0.9951	1.0415	1.1346	-
		S-Type-A						
100	0.5	Present	1.6482	1.7553	1.6006	1.6174	1.5063	1.2839
		3D Elasticity (Li *et al.* 2008)	1.6229	-	1.5817	1.5227	1.5065	1.2655
		% Error	1.559	-	1.195	6.219	-0.013	1.454
	1	Present	1.7924	1.8729	1.7663	1.6939	1.6852	1.3794
		3D Elasticity (Li *et al.* 2008)	1.7916	-	1.7537	1.6818	1.6749	1.3833
		% Error	0.045	-	0.718	0.719	0.615	-0.282
	5	Present	1.9112	1.9918	1.9150	1.8811	1.8895	1.5513
		3D Elasticity (Li *et al.* 2008)	1.9431	-	1.9362	1.8620	1.8853	1.5703
		% Error	-1.642	-	-1.095	1.026	0.223	-1.210
	10	Present	1.9117	1.9919	1.9251	1.9117	1.9195	1.6165
		3D Elasticity (Li *et al.* 2008)	1.9468	-	1.9504	1.8804	1.9116	1.6045
		% Error	-1.803	-	-1.297	1.665	0.413	0.748
10	0.5	Present	1.5292	1.6209	1.4967	1.4789	1.4457	1.2038
		3D Elasticity (Li *et al.* 2008)	1.5258	-	1.4845	1.4341	1.4166	1.2055
		% Error	0.223	-	0.822	3.124	2.054	-0.141
	1	Present	1.6758	1.7243	1.6982	1.5742	1.5588	1.3129
		3D Elasticity (Li *et al.* 2008)	1.6743	-	1.6305	1.5703	1.5578	1.3082
		% Error	0.090	-	4.152	0.248	0.064	0.359
	5	Present	1.8303	1.8451	1.8017	1.7874	1.7633	1.4690
		3D Elasticity (Li *et al.* 2008)	1.8261	-	1.7895	1.7272	1.7267	1.4664
		% Error	0.230	-	0.682	3.485	2.120	0.177
	10	Present	1.8418	1.8579	1.8180	1.7942	1.7751	1.4980
		3D Elasticity (Li *et al.* 2008)	1.8398	-	1.8081	1.7477	1.7481	1.4948
		% Error	0.109	-	0.548	2.661	1.545	0.214

non-dimensional natural frequency increases for H-Type-A plate and decreases for S-Type-A plate. When thickness of core is less, H-type-A plates exhibits less stiff behavior as compared to corresponding S-Type-A plates. But when thickness of core increases, H-Type-A plate shows stiffer behavior as compared to corresponding S-Type-A plate.

Aman Garg et al.

Table 3 Variation of non-dimensional natural frequency for Type-A square shaped (*a/h*=4) sandwich FG plate with different end conditions

Thickness scheme	*n*	CCCC	SSCC	CCCF	CCFF	SSSS	CFFF
			H-Type-A				
2-1-2	0.5	2.0207	1.7078	1.4025	1.3335	1.3520	0.2588
	1	1.8378	1.5374	1.2788	1.2180	1.1915	0.2304
	5	1.4117	1.1612	0.9998	0.9567	0.8830	0.1784
	10	1.3747	1.1561	0.9513	0.9046	0.9033	0.1724
2-1-1	0.5	2.0373	1.7241	1.4136	1.3430	1.3675	0.2613
	1	1.8841	1.5881	1.3003	1.2352	1.2421	0.2348
	5	1.4928	1.2479	1.0361	0.9859	0.9661	0.1855
	10	1.4082	1.1786	0.9836	0.9369	0.9188	0.1796
1-1-1	0.5	2.0583	1.7410	1.4283	1.3573	1.3800	0.2637
	1	1.9137	1.6097	1.3233	1.2578	1.2560	0.2383
	5	1.3714	1.0554	1.0523	1.0203	0.7805	0.1863
	10	1.4166	1.1506	1.0157	0.9725	0.8599	0.1794
2-2-1	0.5	2.0748	1.7558	1.4416	1.3691	1.3926	0.2666
	1	1.9484	1.6420	1.3478	1.2798	1.2851	0.2437
	5	1.6052	1.3346	1.1172	1.0626	1.0229	0.1965
	10	1.5479	1.2940	1.0702	1.0159	0.9948	0.1891
1-2-1	0.5	2.1006	1.7778	1.4606	1.3869	1.4107	0.2704
	1	1.9912	1.6781	1.3798	1.3098	1.3144	0.2499
	5	1.7023	1.4187	1.1783	1.1178	1.0803	0.2050
	10	1.6087	1.3237	1.1327	1.0775	0.9963	0.1970
1-8-1	0.5	2.2255	1.8881	1.5626	1.4798	1.5092	0.2945
	1	2.1770	1.8434	1.5271	1.4458	1.4645	0.2848
	5	2.0611	1.7377	1.4435	1.3652	1.3621	0.2632
	10	2.0399	1.7186	1.4284	1.3506	1.3441	0.2594
			S-Type-A				
2-1-2	0.5	1.7242	1.5177	1.3230	1.2453	1.1755	0.2906
	1	1.8155	1.5979	1.3912	1.3118	1.2375	0.3087
	5	1.9447	1.7035	1.4675	1.4001	1.3205	0.3267
	10	1.9624	1.7158	1.4723	1.4106	1.3305	0.3271
2-1-1	0.5	1.7215	1.5182	1.3233	1.2340	1.1629	0.2851
	1	1.8175	1.6035	1.3939	1.3004	1.2245	0.3020
	5	2.0036	1.7594	1.5091	1.4250	1.3433	0.3232
	10	2.0673	1.8095	1.5434	1.4680	1.3859	0.3265
1-1-1	0.5	1.6563	1.4633	1.2842	1.1989	1.1306	0.2842
	1	1.7195	1.5217	1.3377	1.2471	1.1746	0.3012
	5	1.7985	1.5900	1.3917	1.3040	1.2261	0.3200
	10	1.8083	1.5968	1.3939	1.3099	1.2315	0.3211
2-2-1	0.5	1.6456	1.4553	1.2776	1.1837	1.1146	0.2777
	1	1.7080	1.5136	1.3296	1.2284	1.1549	0.2927
	5	1.7873	1.5844	1.3845	1.2824	1.2032	0.3108
	10	1.7967	1.5911	1.3870	1.2880	1.2083	0.3120

Table 3 Continued

Thickness scheme	n	CCCC	SSCC	CCCF	CCFF	SSSS	CFFF
	0.5	1.5878	1.4068	1.2424	1.1509	1.0848	0.2748
1-2-1	1	1.6282	1.4477	1.2846	1.1842	1.1144	0.2901
	5	1.6684	1.4890	1.3263	1.2179	1.1429	0.3110
	10	1.6699	1.4904	1.3270	1.2193	1.1436	0.3118
	0.5	1.4469	1.2701	1.1052	1.0401	0.9825	0.2333
1-8-1	1	1.4743	1.3015	1.1450	1.0645	1.0043	0.2458
	5	1.5066	1.3440	1.2038	1.0967	1.0318	0.2672
	10	1.5090	1.3481	1.2105	1.0997	1.0341	0.2701

Table 4 Variation of non-dimensional natural frequency for SSSS square-shaped Type-B sandwich FG plate

a/h	n	Source	2-1-2	2-1-1	1-1-1	2-2-1	1-2-1	1-8-1
		CT-Type-B						
		Present	1.3165	1.2482	1.4171	1.4160	1.3544	1.3440
	0.5	3D Elasticity (Li *et al.* 2008)	-	-	-	-	-	1.3393
		% Error						0.351
		Present	1.3451	1.3081	1.3987	1.2146	1.1991	1.3805
	1	3D Elasticity (Li *et al.* 2008)	-	-	-	-	-	1.3866
100		% Error						-0.440
		Present	1.5275	1.5846	1.5495	1.5121	1.5691	1.5478
	5	3D Elasticity (Li *et al.* 2008)	-	-	-	-	-	1.5314
		% Error						1.071
		Present	1.5447	1.5994	1.5651	1.5290	1.5768	1.5964
	10	3D Elasticity (Li *et al.* 2008)	-	-	-	-	-	1.5910
		% Error						0.339
		Present	1.0708	1.0198	1.1679	1.1758	1.1160	1.3107
	0.5	3D Elasticity (Li *et al.* 2008)	-	-	-	-	-	1.2975
		% Error						1.017
		Present	1.2943	1.2707	1.3484	1.1854	1.1600	1.3358
	1	3D Elasticity (Li *et al.* 2008)	-	-	-	-	-	1.3484
10		% Error						-0.934
		Present	1.1755	1.5388	1.3927	1.3741	1.4868	1.4802
	5	3D Elasticity (Li *et al.* 2008)	-	-	-	-	-	1.4930
		% Error						-0.857
		Present	1.5142	1.6318	1.5181	1.4336	1.5315	1.5268
	10	3D Elasticity (Li *et al.* 2008)	-	-	-	-	-	1.5498
		% Error						-1.484
		MT-Type-B						
	0.5	Present	1.3584	1.1408	0.9853	1.1620	1.1873	1.3052
100	1	Present	1.3104	1.1267	1.3542	1.1486	1.2039	1.3741
	5	Present	1.6210	1.5109	1.6707	1.5569	1.6403	1.8250
	10	Present	1.5371	1.3093	1.5895	1.5119	1.6838	1.8990
	0.5	Present	1.2026	1.0889	1.0612	1.1141	1.1470	1.2559
10	1	Present	1.2708	1.1779	1.3040	1.1152	1.2691	1.3276
	5	Present	1.4881	1.2663	1.5285	1.4156	1.5972	1.7713
	10	Present	1.5937	1.3652	1.6470	1.5693	1.7391	1.9406

Table 3 shows the non-dimensional natural frequency for Type-A plates with different end conditions (a/h=4). The minimum value of non-dimensional natural frequency is observed for the CFFF plate for all cases and maximum for the CCCC case as expected. The nature of boundary conditions, along with the thickness scheme, widely affects the free vibration behavior of the plate.

Type-B sandwich FG plate: Table 4 shows values for non-dimensional natural frequency for CT-Type-B and MT-Type-B plates for different thickness schemes and power-law exponent (n). present results are compared with the 3D Elasticity-based results given by Li *et al.* (2008) for a 1-8-1 thickness scheme and are in good agreement. With an increase in the value of n, the value of non-dimensional natural frequency also increases for both Type-B plate types. Due to unsymmetric material distribution across the plate's thickness concerning the reference plane, no definite pattern is observed on the variation of non-dimensional natural frequency as observed for Type-A plate. The value of n and a/h are found to be the important factors governing the variation of non-dimensional natural frequency with change in the thickness of the core. Generally, it increases when the thickness of the core increases from 2-1-2 case to 1-1-1 case and then decreases for CT-Type-B plate, whereas opposite behavior is observed for MT-Type-B plate. plate with higher ceramic content exhibits stiff behavior. Compared to Type-A plate, at lower values of n, Type-B plate shows stiffer behavior, but at higher values of n, Type-A plates exhibit stiffer behavior. Table 5 shows values of non-dimensional natural frequency for the plate with a/h=4 with different end

Table 5 Variation of non-dimensional natural frequency for Type-B square shaped (a/h=4) sandwich FG plate with different end conditions

Thickness scheme	n	CCCC	SSCC	CCCF	CCFF	SSSS	CFFF
				CT-Type-B			
2-1-2	0.5	1.7901	1.5076	1.2458	1.1875	1.1984	0.2320
	1	1.7827	1.5123	1.2255	1.1651	1.2061	0.2293
	5	1.6033	1.3521	1.1344	1.0836	1.0918	0.2229
	10	1.6011	1.3619	1.1194	1.0652	1.1074	0.2217
2-1-1	0.5	1.8788	1.5406	1.3678	1.3137	1.1996	0.2546
	1	1.9552	1.6290	1.3528	1.2133	1.2184	0.2470
	5	1.9222	1.6448	1.2736	1.1987	1.2620	0.2321
	10	1.8944	1.6252	1.2522	1.1775	1.2510	0.2294
1-1-1	0.5	1.9070	1.6231	1.2920	1.2249	1.2798	0.2383
	1	1.8885	1.6149	1.2604	1.1872	1.2580	0.2332
	5	1.5865	1.3468	1.1176	1.0659	1.0949	0.2229
	10	1.5564	1.3304	1.0918	1.0383	1.0944	0.2215
2-2-1	0.5	1.9775	1.6587	1.3946	1.3312	1.3129	0.2601
	1	1.8333	1.5022	1.3341	1.2820	1.1633	0.2498
	5	1.8248	1.5447	1.2122	1.1397	1.1247	0.2274
	10	1.5903	1.3311	1.1386	1.0908	1.0686	0.2236
1-2-1	0.5	1.8986	1.5938	1.3354	1.2727	1.2608	0.2494
	1	1.8525	1.5563	1.2827	1.2159	1.2040	0.2407
	5	1.5571	1.3293	1.0992	1.0477	1.0932	0.2239
	10	1.5072	1.2977	1.0628	1.0096	1.0856	0.2224
1-8-1	0.5	2.0558	1.7431	1.4437	1.3752	1.4040	0.2764
	1	1.8671	1.5726	1.3252	1.2657	1.2603	0.2547
	5	1.5168	1.3051	1.0727	1.0206	1.0903	0.2232
	10	1.4435	1.2529	1.0242	0.9711	1.0682	0.2201

Table 5 Continued

Thickness scheme	n	CCCC	SSCC	CCCF	CCFF	SSSS	CFFF
				MT-Type-B			
2-1-2	0.5	1.7572	1.4978	1.2004	1.2012	1.1395	0.2270
	1	1.7773	1.4730	1.0190	1.2164	1.1652	0.2295
	5	1.8243	1.5356	1.2137	1.2670	1.2065	0.2344
	10	1.8430	1.5543	1.2274	1.2746	1.2124	0.2354
2-1-1	0.5	1.4636	1.2205	1.0062	1.0827	1.0423	0.2218
	1	1.4779	1.2218	1.0044	1.0993	1.0595	0.2217
	5	1.5049	1.2300	1.0056	1.1249	1.0850	0.2215
	10	1.5102	1.2324	1.0065	1.1293	1.0895	0.2216
1-1-1	0.5	1.5377	1.2240	0.9626	1.1823	1.1477	0.2307
	1	1.7991	1.5225	1.2161	1.2445	1.1859	0.2332
	5	1.8988	1.6007	1.2631	1.3144	1.2513	0.2417
	10	1.9217	1.6216	1.2799	1.3286	1.2639	0.2443
2-2-1	0.5	1.5261	1.2717	1.0399	1.1235	1.0824	0.2268
	1	1.6707	1.4007	1.0828	1.1761	1.1229	0.2293
	5	1.7474	1.4549	1.1577	1.2425	1.1896	0.2324
	10	1.8145	1.5250	1.2062	1.2644	1.2050	0.2342
1-2-1	0.5	1.6400	1.3592	1.0922	1.2001	1.1558	0.2344
	1	1.7285	1.4252	1.1304	1.2599	1.2123	0.2398
	5	1.9860	1.6756	1.3256	1.3791	1.3132	0.2545
	10	2.0264	1.7135	1.3591	1.4043	1.3358	0.2597
1-8-1	0.5	1.7144	1.4445	1.1706	1.2317	1.1816	0.2436
	1	1.8494	1.5546	1.2474	1.3181	1.2625	0.2539
	5	2.1457	1.8212	1.4612	1.4949	1.4220	0.2824
	10	2.2062	1.8769	1.5140	1.5381	1.4620	0.2929

conditions. in the case of thick plates, the trend of variation of non-dimensional natural frequency with n can be observed clearly. With an increase in the value of n, the non-dimensional natural frequency decreases for the CT-Type-B plate and increases for the MT-Type-B plate.

Type-S sandwich FG plate: Table 6 shows the non-dimensional natural frequency for the Type-S sandwich FG plate. With an increase in the value of n, the value of non-dimensional natural frequency decreases for the H-Type-S plate and increases for the S-Type-S plate. H-Type-S plate gives a lower value of non-dimensional natural frequency as compared to the S-Type-S plate. With an increase in the core's thickness, non-dimensional natural frequency increases for the H-Type-S plate and decreases for the S-Type-S plate. Table 7 shows the value for the Type-S plate's non-dimensional natural frequency with a/h=4 for different end conditions. The maximum value for the non-dimensional natural frequency is observed for CCCC plate whereas minimum for the CFFF one as expected.

Tables 8-10 show the value of non-dimensional natural frequency for Type-A, B, and S simply supported rhombic plates, respectively (a/h=10). With an increase in the value of the plate's skew angle, non-dimensional natural frequency increases for all the cases. This is because, as the skew angle of the plate is increasing, the influence of the boundary condition towards the central portion of the plate increases and effective length of the plate (projected length of the plate along Y-axis) decreases.

Table 6 Variation of non-dimensional natural frequency for SSSS square-shaped Type-S sandwich FG plate

a/h	n	2-1-2	2-1-1	1-1-1	2-2-1	1-2-1	1-8-1
				H-Type-S			
100	0.5	1.3457	1.4846	1.4687	1.2905	1.5316	1.7465
		1.3555	1.4342	1.4400	1.2596	1.5157	1.7416
	1	1.2748	1.3561	1.3801	1.2012	1.4930	1.7338
		1.2590	1.3546	1.3778	1.1952	1.4963	1.7329
	5	1.3137	1.4445	1.4315	1.1288	1.4925	1.6952
		1.3237	1.3980	1.4048	1.1092	1.4775	1.6907
	10	1.2476	1.3246	1.3484	1.0672	1.4560	1.6831
		1.2323	1.3228	1.3460	1.0620	1.4589	1.6823
				S-Type-S			
10	0.5	1.9487	1.9283	1.9315	1.6347	1.8822	1.5228
		1.9924	1.9633	1.9631	1.6573	1.8979	1.5301
	1	2.0700	2.0014	2.0181	1.6962	1.9245	1.5426
		2.0803	1.9959	2.0232	1.6997	1.9249	1.5443
	5	1.8071	1.7988	1.7746	1.1089	1.7219	1.4260
		1.8358	1.8169	1.7959	1.1084	1.7334	1.4322
	10	1.8669	1.8199	1.8210	1.0820	1.7461	1.4421
		1.8662	1.8075	1.8191	1.0735	1.7433	1.4432

Table 7 Variation of non-dimensional natural frequency for Type-S square shaped (*a/h*=4) sandwich FG plate with different end conditions

Thickness scheme	n	CCCC	SSCC	CCCF	CCFF	SSSS	CFFF
				H-Type-S			
2-1-2	0.5	1.8425	1.5305	1.3043	1.2467	1.1808	0.2394
	1	1.8378	1.5374	1.2788	1.2180	1.1915	0.2304
	5	1.7598	1.4724	1.2112	1.1516	1.1322	0.2133
	10	1.7422	1.4569	1.1997	1.1408	1.1193	0.2111
2-1-1	0.5	1.9232	1.6256	1.3311	1.2645	1.2826	0.2441
	1	1.8928	1.5958	1.3066	1.2413	1.2495	0.2364
	5	1.8319	1.5397	1.2596	1.1964	1.1933	0.2240
	10	1.8264	1.5356	1.2554	1.1922	1.1908	0.2235
1-1-1	0.5	1.9394	1.6322	1.3464	1.2804	1.2789	0.2451
	1	1.9183	1.6138	1.3265	1.2608	1.2598	0.2391
	5	1.8653	1.5670	1.2853	1.2211	1.2155	0.2289
	10	1.8612	1.5637	1.2825	1.2184	1.2131	0.2285
2-2-1	0.5	0.8986	0.6941	0.6576	0.6265	0.6963	0.2020
	1	0.8985	0.6940	0.6562	0.6261	0.6957	0.1992
	5	0.8896	0.6938	0.6474	0.6192	0.6925	0.1928
	10	0.8863	0.6938	0.6450	0.6169	0.6910	0.1919
1-2-1	0.5	2.0109	1.6961	1.3948	1.3243	1.3323	0.2539
	1	1.9988	1.6850	1.3853	1.3150	1.3210	0.2513
	5	1.9764	1.6656	1.3690	1.2995	1.3034	0.2476
	10	1.9774	1.6667	1.3699	1.3004	1.3052	0.2481
1-8-1	0.5	2.2085	1.8721	1.5500	1.4677	1.4923	0.2908
	1	2.2035	1.8677	1.5464	1.4643	1.4886	0.2900
	5	2.1946	1.8601	1.5402	1.4584	1.4822	0.2888
	10	2.1935	1.8592	1.5395	1.4577	1.4815	0.2886

Table 7 Continued

Thickness scheme	n	CCCC	SSCC	CCCF	CCFF	SSSS	CFFF
				S-Type-S			
2-1-2	0.5	1.8360	1.6094	1.3914	1.3225	1.2491	0.3045
	1	1.8155	1.5979	1.3912	1.3118	1.2375	0.3087
	5	1.7101	1.5213	1.3476	1.2456	1.1703	0.3114
	10	1.6805	1.4984	1.3321	1.2261	1.1509	0.3105
2-1-1	0.5	1.8525	1.6269	1.4039	1.3223	1.2475	0.2990
	1	1.8153	1.6008	1.3910	1.2984	1.2227	0.3006
	5	1.7061	1.5155	1.3376	1.2304	1.1549	0.2990
	10	1.6697	1.4853	1.3164	1.2074	1.1327	0.2965
1-1-1	0.5	1.7312	1.5273	1.3352	1.2526	1.1808	0.2977
	1	1.7185	1.5207	1.3368	1.2463	1.1739	0.3008
	5	1.6490	1.4719	1.3130	1.2035	1.1304	0.3029
	10	1.6243	1.4531	1.3012	1.1874	1.1144	0.3020
2-2-1	0.5	0.7076	0.5917	0.5925	0.5274	0.4912	0.1858
	1	0.6999	0.5915	0.5928	0.5223	0.4860	0.1851
	5	0.6671	0.5914	0.5637	0.4993	0.4636	0.1795
	10	0.6592	0.5915	0.5561	0.4937	0.4583	0.1780
1-2-1	0.5	1.6308	1.4471	1.2797	1.1843	1.1150	0.2876
	1	1.6270	1.4462	1.2828	1.1830	1.1134	0.2892
	5	1.5868	1.4186	1.2713	1.1584	1.0885	0.2900
	10	1.5695	1.4055	1.2635	1.1469	1.0773	0.2890
1-8-1	0.5	1.4572	1.2822	1.1209	1.0495	0.9909	0.2384
	1	1.4598	1.2851	1.1246	1.0517	0.9929	0.2394
	5	1.4578	1.2853	1.1283	1.0513	0.9921	0.2407
	10	1.4558	1.2840	1.1282	1.0502	0.9910	0.2408

Table 8 Non-dimensional natural frequency for SSSS Type-A rhombic plate (a/h=10)

Ξ^0	n	2-1-2	2-1-1	1-1-1	2-2-1	1-2-1	1-8-1
				H-Type-A			
15°	0.5	1.6117	1.6318	1.6457	1.6615	1.6831	1.8138
	1	1.3992	1.4659	1.4784	1.5165	1.5509	1.7508
	5	1.0198	1.1323	0.8817	1.1852	1.2479	1.6102
	10	1.0676	1.0847	0.9835	1.1609	1.1428	1.5860
30°	0.5	1.9136	1.9368	1.9534	1.9720	1.9976	2.1519
	1	1.6660	1.7413	1.7566	1.8010	1.8418	2.0777
	5	1.2161	1.3437	1.0552	1.4072	1.4851	1.9119
	10	1.2676	1.2864	1.1777	1.3784	1.3649	1.8834
45°	0.5	2.6427	2.6740	2.6970	2.7225	2.7578	2.9685
	1	2.3080	2.4081	2.4296	2.4901	2.5463	2.8682
	5	1.6851	1.8552	1.4497	1.9448	2.0597	2.6432
	10	1.7514	1.7731	1.6370	1.9058	1.8969	2.6043
60°	0.5	4.6141	4.4506	4.5804	4.5021	4.5766	4.7230
	1	4.0579	4.2333	4.2718	4.3763	4.4750	4.6851
	5	2.9611	3.2573	1.7812	3.4249	3.6364	4.6453
	10	1.6410	3.1016	2.8806	3.3564	3.3531	4.5812

Aman Garg et al.

Table 8 Continued

Ξ^0	n	2-1-2	2-1-1	1-1-1	2-2-1	1-2-1	1-8-1
				S-Type-A			
15°	0.5	1.8221	1.8133	1.7873	1.7684	1.7332	1.4687
	1	1.9342	1.9223	1.8937	1.8685	1.8306	1.5516
	5	2.0440	2.0505	2.0121	1.9868	1.9601	1.6938
	10	2.0456	2.0647	2.0186	1.9938	1.9722	1.7136
30°	0.5	2.1470	2.1375	2.1040	2.0824	2.0396	1.7325
	1	2.2776	2.2658	2.2267	2.1984	2.1511	1.8281
	5	2.4060	2.4198	2.3618	2.3340	2.2969	1.9909
	10	2.4081	2.4397	2.3689	2.3416	2.3099	2.0134
45°	0.5	2.9074	2.8998	2.8447	2.8198	2.7565	2.3578
	1	3.0794	3.0719	3.0023	2.9708	2.8976	2.4810
	5	3.2506	3.2866	3.1720	3.1428	3.0749	2.6870
	10	3.2542	3.3237	3.1802	3.1516	3.0891	2.7147
60°	0.5	3.2702	3.4012	3.2682	3.3386	3.2327	0.2890
	1	3.4428	3.6071	3.4341	3.5257	3.3895	3.0000
	5	3.7399	3.9714	3.7095	3.8328	3.6595	3.2104
	10	3.7994	4.0693	3.7597	3.8860	3.7051	3.2431

Table 9 Non-dimensional natural frequency for SSSS Type-B rhombic plate (*a/h*=10)

Ξ^0	n	2-1-2	2-1-1	1-1-1	2-2-1	1-2-1	1-8-1
				CT-Type-B			
15°	0.5	1.4467	1.3919	1.5632	1.5567	1.4943	1.6991
	1	1.4746	1.5635	1.5853	1.3572	1.4440	1.5141
	5	1.3439	1.5351	1.3623	1.4039	1.3771	1.3915
	10	1.3857	1.5263	1.3896	1.2990	1.4035	1.3987
30°	0.5	1.7154	1.6463	1.8829	1.8432	1.7715	2.1023
	1	1.7573	0.9891	1.7875	1.6104	1.7374	1.7914
	5	1.5858	1.8646	1.6085	1.7513	1.6256	1.6433
	10	1.6388	1.8511	1.6424	1.5302	1.6578	1.6519
45°	0.5	2.3629	2.2558	2.3221	2.5341	2.4400	2.7663
	1	2.4329	0.7077	1.3888	2.2170	2.4353	2.4579
	5	2.1661	2.6306	2.1983	1.6337	2.2199	2.2444
	10	2.2449	2.6094	2.2463	2.0845	2.2633	2.2538
60°	0.5	3.6545	3.9187	2.0402	4.4167	4.2626	4.7779
	1	2.9378	0.5614	1.1375	3.4796	2.8932	4.2629
	5	3.7251	2.4915	3.7770	1.3520	3.8026	3.4586
	10	3.8627	2.5747	3.7481	3.5788	3.4828	3.0923
				MT-Type-B			
15°	0.5	1.4902	1.2501	1.1150	1.2772	1.3124	1.4286
	1	1.4825	1.2383	1.4857	1.2845	1.3364	1.5047
	5	1.4541	1.2261	1.5078	1.3866	1.5800	1.7637
	10	1.4710	1.2250	1.5274	1.4446	1.6245	1.8368
30°	0.5	1.7875	1.4662	1.3039	1.4996	1.5435	1.6853
	1	1.7551	1.4518	1.7709	1.5287	1.5740	1.7776
	5	1.7237	1.4371	1.7889	1.6380	1.8738	2.0912
	10	1.7451	1.4358	1.8127	1.7115	1.9278	2.1780

Table 9 Continued

Ξ^0	n	2-1-2	2-1-1	1-1-1	2-2-1	1-2-1	1-8-1
45°	0.5	2.4812	1.9821	1.7534	2.0309	2.0967	2.3003
	1	2.4593	1.9617	2.4492	2.1147	2.1438	2.4334
	5	2.3746	1.9418	2.4680	2.2435	2.5839	2.8811
	10	2.4069	1.9402	2.5021	2.3556	2.6604	3.0003
60°	0.5	2.1939	3.4655	2.9734	3.4541	3.5914	3.6681
	1	3.2557	3.3195	2.6054	3.7111	3.6922	3.9744
	5	4.1446	3.2946	4.2420	3.8867	4.4729	4.5333
	10	4.2068	3.2927	4.3758	4.1073	4.4671	4.6410

Table 10 Non-dimensional natural frequency for SSSS Type-S rhombic plate (a/h=10)

Ξ^0	n	2-1-2	2-1-1	1-1-1	2-2-1	1-2-1	1-8-1
			H-Type-S				
15°	0.5	1.3908	1.5251	1.5120	1.1947	1.5757	1.7893
	1	1.3992	1.4760	1.4835	1.1745	1.5599	1.7845
	5	1.3179	1.3988	1.4238	1.1308	1.5372	1.7765
	10	1.3019	1.3969	1.4212	1.1253	1.5402	1.7756
30°	0.5	1.6615	1.8109	1.7970	1.4210	1.8712	2.1231
	1	1.6660	1.7532	1.7625	1.3990	1.8524	2.1174
	5	1.5672	1.6623	1.6915	1.3497	1.8255	2.1080
	10	1.5486	1.6602	1.6884	1.3433	1.8290	2.1069
45°	0.5	2.3058	2.5021	2.4851	1.9181	2.5861	2.9297
	1	2.3080	2.4241	2.4377	1.8932	2.5606	2.9219
	5	2.1711	2.3012	2.3405	1.8330	2.5238	2.9089
	10	2.1457	2.2985	2.3362	1.8244	2.5285	2.9075
60°	0.5	4.0429	4.3532	4.3623	2.1371	4.5401	4.7064
	1	4.0579	4.2600	4.2855	2.1297	4.4989	4.7053
	5	3.8305	4.0549	4.1223	2.1133	4.4364	4.7039
	10	3.7861	4.0499	4.1145	2.1086	4.4438	4.7035
			S-Type-S				
15°	0.5	1.9045	1.8963	1.8692	1.1598	1.8130	1.5024
	1	1.9342	1.9146	1.8912	1.1586	1.8249	1.5089
	5	1.9646	1.9159	1.9162	1.1289	1.8356	1.5193
	10	1.9633	1.9022	1.9138	1.1197	1.8383	1.5204
30°	0.5	2.2451	2.2386	2.1997	1.3316	2.1313	1.7714
	1	2.2776	2.2570	2.2240	1.3280	2.1447	1.7789
	5	2.3049	2.2516	2.2478	1.2873	2.1568	1.7907
	10	2.3013	2.2335	2.2436	1.2753	2.1591	1.7918
45°	0.5	3.0427	3.0447	2.9709	1.6992	2.8734	2.4078
	1	3.0794	3.0610	2.9989	1.6900	2.8898	2.4177
	5	3.0927	3.0338	3.0161	1.6248	2.8988	2.4324
	10	3.0821	3.0044	3.0065	1.6071	2.8995	2.4336
60°	0.5	3.4095	3.6095	3.4003	1.7265	3.3679	2.9405
	1	3.4428	3.6018	3.4280	1.7339	3.3781	2.9427
	5	3.5939	3.6708	3.5273	1.7641	3.4182	2.9463
	10	3.6354	3.6945	3.5503	1.7687	3.4232	2.9464

Aman Garg et al.

4. Conclusions

In present work, free vibration analysis of sandwich FG plates is carried out using recently proposed higher-order zigzag theory. Comparative study has been carried out between different kinds of power-law and sigmoidal sandwich FG plates. It has been observed that the power-law exponent and thickness scheme widely determine the free vibration behavior of the plate. in most of the cases, power-law plate outperforms the sigmoidal sandwich FG plate. Boundary condition and skew angle also affects the vibration behavior of the plate.

• Plate with higher content of ceramic content exhibits higher value for non-dimensional natural frequency due to more inertia of ceramic phase used during the present study.

• CFFF plate exhibits lowest value for the non-dimensional natural frequency, whereas the CCCC plate shows the highest value.

• For Type-A plate with value of $n \leq 1$, H-Type-A plate shows higher value for non-dimensional natural frequency as compared to S-type-A plate for all boundary conditions. Opposite trend is observed when the value of $n > 1$. In this respect, the behavior of CT-Type-B plate is similar to H-Type-A plate and MT-Type-B plate is similar to S-Type-A plate. The behavior of H- and S-Type-S plates for different values of n depends widely on its boundary condition.

• Increasing the skew angle of the plate, non-dimensional natural frequency increases as the influence of the boundary conditions towards the central portion increases.

Acknowledgments

References

Apetre, N.A., Sankar, B.V. and Ambur, D.R. (2008), "Analytical modeling of sandwich beams with functionally graded core", *J. Sandw. Struct. Mater.*, **10**, 53-74. https://doi.org/10.1177/1099636207081111.

Bacciocchi, M., Eisenberger, M., Fantuzzi, N., Tornabene, F. and Viola, E. (2016), "Vibration analysis of variable thickness plates and shells by the generalized differential quadrature method", *Compos. Struct.*, **156**, 218-237. https://doi.org/10.1016/j.compstruct.2015.12.004.

Belalia, S.A. (2019), "A new analysis of nonlinear free vibration behavior of bi-functionally graded sandwich plates using the p-version of the finite element method", *Mech. Adv. Mater. Struct.*, **26**, 727-740. https://doi.org/10.1080/15376494.2017.1410912.

Bennoun, M., Houari, M.S.A. and Tounsi, A. (2016), "A novel five-variable refined plate theory for vibration analysis of functionally graded sandwich plates", *Mech. Adv. Mater. Struct.*, **23**, 423-431. https://doi.org/10.1080/15376494.2014.984088.

Birman, V. and Bert, C.W. (2002), "On the choice of shear correction factor in sandwich structures", *J. Sandw. Struct. Mater.*, **4**, 83-95. https://doi.org/10.1177/1099636202004001180.

Bouafia, K., Selim, M.M., Bourada, F., Bousahla, A.A., Bourada, M., Tounsi, A., Bedia E.A.A. and Tounsi, A. (2021), "Bending and free vibration characteristics of various compositions of FG plates on elastic foundation via quasi 3D HSDT model", *Steel Compos. Struct.*, **41**(4), 487-503. https://doi.org/10.12989/scs.2021.41.4.487.

Brischetto, S. (2009), "Classical and mixed advanced models for sandwich plates embedding functionally graded cores", *J. Mech. Mater. Struct.*, **4**, 13-33. https://doi.org/10.2140/jomms.2009.4.13.

Burlayenko, V.N. and Sadowski, T. (2020), "Free vibrations and static analysis of functionally graded sandwich plates with three-dimensional finite elements", *Meccanica*, **55**, 815-832. https://doi.org/10.1007/s11012-019-01001-7.

Carrera, E. (2003), "Historical review of Zig-Zag theories for multilayered plates and shells", *Appl. Mech. Rev.*, **56**, 287-308. https://doi.org/10.1115/1.1557614.

Carrera, E., Brischetto, S., Cinefra, M. and Soave, M. (2011), "Effects of thickness stretching in functionally graded plates and shells", *Compos. Part B Eng.*, **42**, 123-133. https://doi.org/10.1016/j.compositesb.2010.10.005.

Chalak, H.D., Chakrabarti, A., Iqbal, M.A. and Sheikh, A.H. (2012), "An improved C0 FE model for the analysis of laminated sandwich plate with softcore", *Finite Elem. Anal. Des.*, **56**, 20-31. https://doi.org/10.1016/j.finel.2012.02.005.

Chalak, H.D., Chakrabarti, A., Iqbal, M.A. and Sheikh, A.H. (2014), "C0 FE model based on HOZT for the analysis of laminated soft core skew sandwich plates: Bending and vibration", *Appl. Math. Model.*, **38**, 1211-1223. http://doi.org/10.1016/j.apm.2013.08.005.

Chanda, A. and Sahoo, R. (2021), "Static and dynamic responses of simply supported sandwich plates using non-polynomial zigzag theory", *Struct.*, **29**, 1911-1933. https://doi.org/10.1016/j.istruc.2020.11.062.

Chen, C.D. and Su, P.W. (2021), "An analytical solution for vibration in a functionally graded sandwich beam by using the refined zigzag theory", *Acta Mech.*, **232**, 4645-4668. http://doi.org/10.1007/s00707-021-03063-9.

Daouadji, T.H., Adim, B. and Benferhat, R. (2016), "Bending analysis of an imperfect FGM plates under hygro-thermo-mechanical loading with analytical validation", *Adv. Mat. Res.*, **5**(1), 35-53. https://doi.org/10.12989/amr.2016.5.1.035.

Di Sciuva, M. and Sorrenti, M. (2019), "Bending and free vibration analysis of functionally graded sandwich plates: An assessment of the Refined Zigzag Theory", *J. Sandw. Struct. Mater.*, **23**(3), 760-802. https://doi.org/10.1177/1099636219843970.

Dorduncu, M. (2020), "Stress analysis of sandwich plates with functionally graded cores using peridynamic differential operator and refined zigzag theory", *Thin Wall. Struct.*, **146**, 106468. https://doi.org/10.1016/j.tws.2019.106468.

Ferreira, A.J.M., Viola, E., Tornabene, F., Fantuzzi, N. and Zenkour, A.M. (2013), "Analysis of sandwich plates by generalized differential quadrature method", *Math. Probl. Eng.*, **2013**, Article ID 964367. https://doi.org/10.1155/2013/964367.

Fu, T., Chen, Z., Yu, H., Wang, Z. and Liu, X. (2020), "Free vibration of functionally graded sandwich plates based on nth-order shear deformation theory via differential quadrature method", *J. Sandw. Struct. Mater.*, **22**(5), 1660-1680. https://doi.org/10.1177/1099636218809451.

Garg, A. and Chalak, H.D. (2019), "A review on analysis of laminated composite and sandwich structures under hygrothermal conditions", *Thin Wall. Struct.*, **142**, 205-226. https://doi.org/10.1016/j.tws.2019.05.005.

Garg, A. and Chalak, H.D. (2021a), "Analysis of non-skew and skew laminated composite and sandwich plates under hygro-thermo-mechanical conditions including transverse stress variations", *J. Sandw. Struct. Mater.*, **23**(8), 3471-3494. https://doi.org/10.1177/1099636220932782.

Garg, A. and Chalak, H.D. (2021b), "Novel higher-order zigzag theory for analysis of laminated sandwich beams", *Proc. Inst. Mech. Eng. Part L J. Mater. Des. Appl.*, **235**(1), 176-194. https://doi.org/10.1177/1464420720957045.

Garg, A., Belarbi, M.O., Chalak, H.D. and Chakrabarti, A. (2021a), "A review of the analysis of sandwich FGM structures", *Compos. Struct.*, **258**, 113427. https://doi.org/10.1016/j.compstruct.2020.113427.

Garg, A., Chalak, H.D. and Chakrabarti, A. (2020a), "Bending analysis of functionally graded sandwich plates using HOZT including transverse displacement effects", *Mech. Bas. Des. Struct. Mach.*, **50**(10), 3563-3577. https://doi.org/10.1080/15397734.2020.1814157.

Garg, A., Chalak, H.D. and Chakrabarti, A. (2020b), "Comparative study on the bending of sandwich FGM beams made up of different material variation laws using refined layerwise theory", *Mech. Mater.*, **151**, 103634. https://doi.org/10.1016/j.mechmat.2020.103634.

Garg, A., Chalak, H.D., Belarbi, M.O. and Zenkour, A.M. (2021b), "Hygro-thermo-mechanical based

bending analysis of symmetric and unsymmetric power-law, exponential and sigmoidal FG sandwich beams", *Mech. Adv. Mater. Struct.*, **29**(25), 4523-4545. https://doi.org/10.1080/15376494.2021.1931993.

Garg, A., Chalak, H.D., Belarbi, M.O., Chakrabarti, A. and Houari, M.S.A. (2021c), "Finite element-based free vibration analysis of power-law, exponential and sigmoidal functionally graded sandwich beams", *J. Inst. Eng. India Ser. C*, **102**(5), 1167-1201. https://doi.org/10.1007/s40032-021-00740-5.

Ghatage, P.S., Kar, V.R. and Sudhagar, P.E. (2020), "On the numerical modelling and analysis of multi-directional functionally graded composite structures: A review", *Compos. Struct.*, **236**, 111837. https://doi.org/10.1016/j.compstruct.2019.111837.

Hadji, L. and Bernard, F. (2020), "Bending and free vibration analysis of functionally graded beams on elastic foundations with analytical validation", *Adv. Mater. Res.*, **9**(1), 63-98. https://doi.org/10.12989/amr.2020.9.1.063.

Hadji, L., Amoozgar, M. and Tounsi, A. (2022), "Non-linear thermal buckling of FG plates with porosity", *Steel Compos. Struct.*, **42**(5), 711-722. https://doi.org/10.12989/scs.2022.42.5.711.

Hadji, L., Atmane, H.A., Tounsi, A., Mechab, I. and Bedia, E.A.A. (2011), "Free vibration of functionally graded sandwich plates using four-variable refined plate theory", *Appl. Math. Mech.*, **32**, 925-942. https://doi.org/10.1007/s10483-011-1470-9.

Hadji, L., Bernard, F., Safa, A. and Tounsi, A. (2021), "Bending and free vibration analysis for FGM plates containing various distribution shape of porosity", *Adv. Mater. Res.*, **10**(2), 115-135. https://doi.org/10.12989/amr.2021.10.2.115.

Iurlaro, L., Gherlone, M. and Di Sciuva, M. (2014), "Bending and free vibration analysis of functionally graded sandwich plates using the Refined Zigzag Theory", *J. Sandw. Struct. Mater.*, **16**(6), 669-699. https://doi.org/10.1177/1099636214548618.

Keddouri, A., Hadji, L. and Tounsi, A. (2019), "Static analysis of functionally graded sandwich plates with porosities", *Adv. Mater. Res.*, **8**(3), 155-177. https://doi.org/10.12989/amr.2019.8.3.155.

Kurpa, L.V. and Shmatko, T.V. (2021), "Buckling and free vibration analysis of functionally graded sandwich plates and shallow shells by the Ritz method and the R-functions theory", *Proc. Inst. Mech. Eng. Part C J. Mech. Eng. Sci.*, **235**(20), 4582-4593. https://doi.org/10.1177/0954406220936304.

Li, Q., Iu, V.P. and Kou, K.P. (2008), "Three-dimensional vibration analysis of functionally graded material sandwich plates", *J. Sound Vib.*, **311**, 498-515. https://doi.org/10.1016/j.jsv.2007.09.018.

Liu, M., Cheng, Y. and Liu, J. (2015), "High-order free vibration analysis of sandwich plates with both functionally graded face sheets and functionally graded flexible core", *Compos. Part B Eng.*, **72**, 97-107. https://doi.org/10.1016/j.compositesb.2014.11.037.

Mahi, A., Bedia, E.A.A. and Tounsi, A. (2015), "A new hyperbolic shear deformation theory for bending and free vibration analysis of isotropic, functionally graded, sandwich and laminated composite plates", *Appl. Math. Model.*, **39**, 2489-2508. https://doi.org/10.1016/j.apm.2014.10.045.

Meksi, R., Benyoucef, S., Mahmoudi, A., Tounsi, A., Bedia, E.A.A. and Mahmoud, S.R. (2019), "An analytical solution for bending, buckling and vibration responses of FGM sandwich plates", *J. Sandw. Struct. Mater.*, **21**, 727-757. https://doi.org/10.1177/1099636217698443.

Neves, A.M.A., Ferreira, A.J.M., Carrera, E., Cinefra, M., Jorge, R.M.N. and Soares, C.M.M. (2012), "Static analysis of functionally graded sandwich plates according to a hyperbolic theory considering Zig-Zag and warping effects", *Adv. Eng. Softw.*, **52**, 30-43. https://doi.org/10.1016/j.advengsoft.2012.05.005.

Neves, A.M.A., Ferreira, A.J.M., Carrera, E., Cinefra, M., Jorge, R.M.N., Soares, C.M.M. and Araújo, A.L. (2017), "Influence of zig-zag and warping effects on buckling of functionally graded sandwich plates according to sinusoidal shear deformation theories", *Mech. Adv. Mater. Struct.*, **24**, 360-376. https://doi.org/10.1080/15376494.2016.1191095.

Neves, A.M.A., Ferreira, A.J.M., Carrera, E., Cinefra, M., Roque, C.M.C., Jorge, R.M.N. and Soares, C.M.M. (2013), "Static, free vibration and buckling analysis of isotropic and sandwich functionally graded plates using a quasi-3D higher-order shear deformation theory and a meshless technique", *Compos. Part B Eng.*, **44**, 657-674. https://doi.org/10.1016/j.compositesb.2012.01.089.

Pai, P.F. (1995), "A new look at shear correction factors and warping functions of anisotropic laminates", Int. *J. Solid. Struct.*, **32**, 2295-2313. https://doi.org/10.1016/0020-7683(94)00258-X.

Pandey, S. and Pradyumna, S. (2015), "Free vibration of functionally graded sandwich plates in thermal

environment using a layerwise theory", *Eur. J. Mech. A/Solid.*, **51**, 55-66. https://doi.org/10.1016/j.euromechsol.2014.12.001.

Patni, M., Minera, S., Groh, R.M.J., Pirrera, A. and Weaver, P.M. (2018), "Three-dimensional stress analysis for laminated composite and sandwich structures", *Compos. Part B Eng.*, **155**, 299-328. https://doi.org/10.1016/j.compositesb.2018.08.127.

Saad, M., Hadji, L. and Tounsi, A. (2021), "Effect of porosity on the free vibration analysis of various functionally graded sandwich plates", *Adv. Mater. Res.*, **10**(4), 293-311. https://doi.org/10.12989/amr.2021.10.4.293.

Sayyad, A.S. and Ghugal, Y.M. (2019), "Modeling and analysis of functionally graded sandwich beams: a review", *Mech. Adv. Mater. Struct.*, **26**, 1776-1795. https://doi.org/10.1080/15376494.2018.1447178.

Singh, S.J. and Harsha, S.P. (2020), "Nonlinear Vibration analysis of sigmoid functionally graded sandwich plate with ceramic-FGM-metal layers", *J. Vib. Eng. Technol.*, **8**, 67-84. https://doi.org/10.1007/s42417-018-0058-8.

Tahir, S.I., Tounsi, A., Chikh, A., Al-Osta1 M.A., Al-Dulaijan S.U. and Al-Zahrani, M.M. (2022), "The effect of three-variable viscoelastic foundation on the wave propagation in functionally graded sandwich plates via a simple quasi-3D HSDT", *Steel Compos. Struct.*, **42**(2), 501-511. https://doi.org/10.12989/scs.2022.42.4.501.

Thai, H.T., Nguyen, T.K., Vo, T.P. and Lee, J. (2014), "Analysis of functionally graded sandwich plates using a new first-order shear deformation theory", *Eur. J. Mech. A/Solid.*, **45**, 211-225. https://doi.org/10.1016/j.euromechsol.2013.12.008.

Tornabene, F. (2009, "Free vibration analysis of functionally graded conical, cylindrical shell and annular plate structures with a four-parameter power-law distribution", *Comput. Meth. Appl. Mech. Eng.*, **198**, 2911-2935. https://doi.org/10.1016/j.cma.2009.04.011.

Tornabene, F., Fantuzzi, N., Ubertini, F. and Viola, E. (2015), "Strong formulation finite element method based on differential quadrature: A survey", *Appl. Mech. Rev.*, **67**, 1-55. https://doi.org/10.1115/1.4028859.

Ye, R., Zhao, N., Yang, D., Cui, J., Gaidai, O. and Ren, P. (2021), "Bending and free vibration analysis of sandwich plates with functionally graded soft core, using the new refined higher-order analysis model", *J. Sandw. Struct. Mater.*, **23**(2), 680-710. https://doi.org/10.1177/1099636220909763.

Zenkour, A., Mashat, D. and Elsibai, K. (2009), "Bending analysis of functionally graded plates in the context of different theories of thermoelasticity", *Math. Prob. Eng.*, **2009**, Article ID 962351. https://doi.org/10.1155/2009/962351.

Zenkour, A.M. (2005a), "A comprehensive analysis of functionally graded sandwich plates: Part 1-Deflection and stresses", *Int. J. Solid. Struct.*, **42**, 5224-5242. https://doi.org/10.1016/j.ijsolstr.2005.02.015.

Zenkour, A.M. (2005b), "A comprehensive analysis of functionally graded sandwich plates: Part 2-Buckling and free vibration", *Int. J. Solid. Struct.*, **42**, 5243-5258. https://doi.org/10.1016/j.ijsolstr.2005.02.016.

Zenkour, A.M. (2006), "Generalized shear deformation theory for bending analysis of functionally graded plates", *Appl. Math. Model.*, **30**, 67-84. https://doi.org/https://doi.org/10.1016/j.apm.2005.03.009.

Zenkour, A.M. (2009), "The effect of transverse shear and normal deformations on the thermomechanical bending of functionally graded sandwich plates", *Int. J. Appl. Mech.*, **1**, 667-707. https://doi.org/10.1142/S1758825109000368.

Zhang, N., Khan, T., Guo, H., Shi, S., Zhong, W. and Zhang, W. (2019), "Functionally graded materials: an overview of stability, buckling, and free vibration analysis", *Adv. Mater. Sci. Eng.*, **2019**, Article ID 1354150. https://doi.org/10.1155/2019/1354150.

Zouatnia, N. and Hadji, L. (2019), "Static and free vibration behavior of functionally graded sandwich plates using a simple higher order shear deformation theory", *Adv. Mater. Res.*, **8**(4), 313-335. https://doi.org/10.12989/amr.2019.8.4.313.